A 3D MICRO-PLANE MODEL FOR SHAPE MEMORY ALLOYS

A. Roohbakhsh Davaran* and S.A. Sadrnejad

Department of Civil Engineering, K.N. Toosi University of Technology
P.O. Box 15875-4416, Tehran, Iran
arash_roohbakhsh@yahoo.com - sadrnejad@kntu.ac.ir

*Corresponding Author

(**Received: October 8, 2007 - Accepted in Revised Form: November 22, 2007)**

Abstract To assess the thermo-mechanical behavior of shape memory alloys and analyzing these special materials, a simple constitutive integrated model, named micro-plane, is proposed. The model deals with shear and normal on plane stress/strain components and also on plane shear orientation as well. The proposed simple model is capable of predicting three-dimensional behavior as the superposition of on plane elastic and inelastic deformations. In the case of static constraint, two on plane stress/strain components and corresponding orientations could be obtained by transferring the stress/strain tensor. Then to calculate the on plane deformations, a plane constitutive law is needed to assess unknown strains/stresses. To represent the capability of this model, the predicted different test data across time and temperature domains are compared with the experimental results. In these test results the shape memory alloys behavior as: super elasticity under various temperatures, loading rate effects, asymmetry in tension and pressure, various loops of loading and unloading, hydrostatic pressure effects, different proportional tension-shear biaxial loading and unloading and also deviation from normality due to non-proportional tension-shear biaxial loading and unloading, are investigated and presented. The interesting well accuracy of results proves the strength and capability of the proposed model.

Keywords Shape Memory Alloys, Shape Memory Effect, Super Elasticity, Micro-Plane, Multi-Laminate

چکیده به منظور بررسی رفتار ترمومکانیکی آلیاژهای حافظه دار و امکان تحلیل عددی این مواد خاص یک الگوی رفتاری ساده بر اساس روش ریز صفحه ای براساس تنها دو مولفه عمود و برش و امتداد مولفه برش در ریز صفحه و روابط بین آنها ارائه شده است. الگوی ارائه شده می‌تواند رفتار سه بعدی یک نقطه را به وسیله جمع آثار غیر خطی تغییر شکل در چندین صفحه با زوایای مختلف پیش بینی کند. در حالت قید استاتیکی نیروهای موجود در هر ریزصفحه از انتقال تانسور تنش در همان ریز صفحه به دست می‌آید سپس برای محاسبه نرخ تغییر شکل در هر ریزصفحه فقط یک قانون رفتاری لازم می‌باشد. برای ارزیابی توانایی و قابلیت این الگو نتایج تحلیلی و تجربی با هم مقایسه شده است. در این نتایج توانایی الگو در ارایه حافظه داری وخاصیت ما فوق ارتجاعی در دماهای مختلف – تاثیر نرخ بارگذاری – نا متقارنی در فشار و کشش – تشکیل حلقه های داخلی در اثر بارگذاری و باربرداری در بار گذاری های یک محوری و اثر فشار هیدرواستاتیک و رفتار این مواد تحت بارگذاری دو محوری کششی و برشی متناسب و همچنین خاصیت انحراف از تعامد در اثر بارگذاری چند محوری نا متناسب دربار گذاری های چند محوری با نتایج تجربی مقایسه شده است که نشان می‌دهد نتایج به دست آمده از این الگو، هم خوانی خوبی با نتایج تجربی دارند. الگوی پیشنهادی، رفتار سازه های ساخته شده از فلزات حافظه دار را در چرخه اعمال تغییر شکل ها می‌تواند به طور مناسبی پیش بینی نماید.

1. INTRODUCTION

Nowadays, civil engineers in addition to taking the factors such as capability of the structure for enduring different loads into account, pay special attention to designing more precise structures with larger spans or reducing the mass of constructional materials in order to economic justification of their projects. Maintenance and reinforcement of the existing buildings is one of the most responsibilities of civil engineers.

The issue of intelligent structures and intelligent

control systems has engaged researchers worldwide. To this end, civil engineers are after using constructional materials with better specifications than the ones currently used. Shape memory alloys are one of such materials which are also called intelligent materials. Although these materials have been known decades ago, but they have been used in the building construction recently. These materials like many other metals have more than one crystal structure which is called poly crystal. The shape of crystal structure in these materials is dependent on temperature and external tension imposed on them [1].

The structural phases in high and low temperatures are respectively called austenite and martensite. The ability to transform into each other in different tensions and temperatures and consequently change of mechanical and electrical properties of these materials has encouraged researchers to use these alloys in smart structures.

To date, some 30 types of these alloys have been known, but due to the common temperature of structures and observing economic justification issues, only some of them are applicable [1].

The ability of returning into the initial shape through increasing the temperature after pseudo plasticity transformations in low temperature phases is one of the most distinctive features of these alloys. To this reason, these alloys are called shape memory alloys and this phenomenon is called pseudo plasticity [1].

Another notable phenomenon is super elasticity which is also called pseudo elasticity. Increase of the tension imposed on material in fixed temperature will turn the austenite phase into martensite phase and after unloading the martensite phase will be turned into austenite phase. The high capacity for energy damping in hysteretic loops is another feature of these alloys. For further study on application of these alloys in building construction industry, refer to [1].

So, analysis of these materials is of high importance in designing and for analysis of the structures in which these alloys have been utilized, a suitable behavioral constitutive law is required.

A three-dimensional model based on the micro-plane integrated method has been proposed as a more capable model predicting the special behavioral aspects of memory alloys in this paper. In continuation, first, the micro-plane method has been described, then the on plane constitutive law cast in micro-plane framework has been introduced and in the next section, comparison of the predicted results with experiments have been presented.

2. MICRO-PLANE MODEL

2.1. Brief History This model was initially proposed by Taylor [2]. He suggested that the constitutive behavior of polycrystalline metals are explained by the relations between strain and tension vectors in planes with different orientations in which the macroscopic stress and strain tensors are obtained by sum of all the vectors in these planes using some static and kinematic constraints and formula. Batdorf, et al [3] were the first individuals who expanded the idea of Taylor and developed a realistic model for plasticity properties of polycrystalline alloys. Many other researchers have modified this method for alloys. Meanwhile, this method has been used for development of the non-linear hardening properties in soils and stones. Micro-plane is referred to a plane in materials with different orientation which is used for estimation of the microstructure behavior of materials. After extension of the micro-plane model by Prat, et al [4] for estimation of damages arising from compression and tension, a very more effective formula for concrete was introduced by Bazant [5,6].

The micro-plane formula for anisotropic clays and for soils has been introduced by Prat, et al in [7-9], respectively.

Details of micro-plane formula in both static and kinematic constraints can be seen in the studies of Bazant, et al [10]. For each formula, in static and kinematic constraints, properties of material are identified by using stress and strain relations in micro-planes.

2.2. The Model Specifications The micro-plane framework is to asset the model assessment between macroscopic and microscopic scale due to the possibility of choosing little or high number in the main numerical integrand as sampling planes. The micro-plane model is based on a

phenomenological model which aims to obtain the mechanical macroscopic behavior of materials divided into sampling plane behaviors. Accordingly, the constitutive law is defined based on plane stress/strain tensors; while in a micro-plane investigate material behavior in several planes with different orientations which are called micro-plane, so that this method is much closer to fit the assessment of mechanical behavior of a group of crystals with multi side reactions instead.

For an isotropic material, the constitutive laws in micro-planes can be considered equal for different planes as well as material parameters. Although, we should note that the number and orientation of micro-planes are obtained using numerical methods and the micro-planes should not be necessarily based on crystallographic structure of materials (like some microstructure mechanical models), but it is possible to select micro-planes according to the planes with known orientation based on crystallographic for a shape memory alloy and apply micro-plane model directly in single crystal microstructure scale [11].

Overall behavior of polycrystalline materials is the sum of shear effects in the planes with different orientation related to the single crystal grains [11]. In macro-scale or polycrystalline scale, the micro-plane model is used as a method with the ability to be turned from a constitutive law in each micro-plane to a three-dimensional macro-scale model for stress-strain tensor. In this case, orientation of micro-planes can be selected using numerical considerations.

Below considerations have been assumed for facilitating the development of the model:

- Negligibility of thermal expansion
- Elasticity of volumetric strain

For obtaining shear strains and their orientations in the micro-plane, it is required that a constitutive law to be defined in each micro-plane. In this model defines a 2-D thermo-mechanic phase transformation surface for on planes constitutive law.

The martensitic strain tensor in macro-scale are due to summation of shear displacement in micro-scale between grains [11], so a constitutive law for each micro-plane has been considered which its 2-D phase transformation surfaces are dependent on the shear direction and the vertical component in the micro-planes (Figure 1,2).

Because the martensite strain related to the phase transformation are high, kinematic constraints in micro-plane models cause constraints and are not suitable. So, static constraint method has been used for obtaining the micro-plane models [11], i.e. by transforming stress tensor in each micro-plane, the vertical and shear component relating to the micro-plane are obtained and using the constitutive law, the rate of vertical and shear strain are obtained in each micro-plane and by superposing of the effects of these plane strains based on the virtual work principle, the overall strain tensor is obtained.

The proposed micro-plane constitutive law has been developed upon modification of the one-dimensional constitutive law presented by

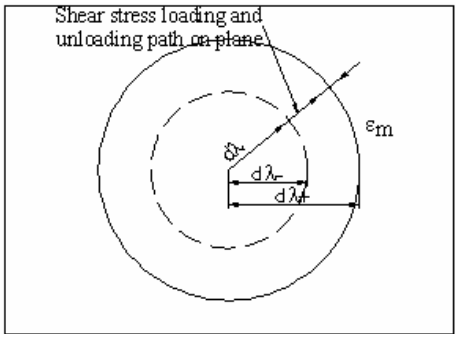

Figure 1. The shear stress path in a micro-plane in the proportional loading and unloading cases and thermo-mechanical borders of crystal phase transformation.

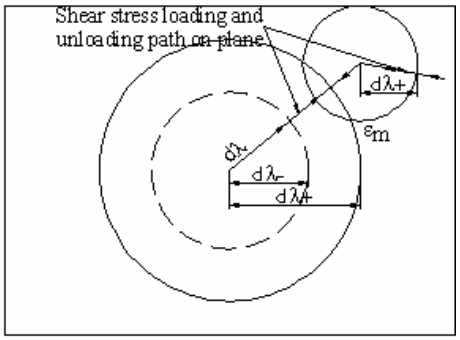

Figure 2. The shear stress path in a micro-plane in the non-proportional loading and unloading cases and thermo-mechanical borders of crystal phase transformation.

Sadjadpour, et al [12,19,20] and applied some amendments to change it into a 3-D constitutive law.

The main advantage of this model is the possibility of definition of independent constitutive law for each micro-plane. Also, the model has the capacity to describe complicated phenomena like deviate from normality that can not be described by using macro-scale models based on associated flow rule or J2 invariant [11]. For example, McDawell, et al [13] experimentally showed that the constitutive laws which are based on J2 such as the yielding surface of Von Mises and Drucker Prager are not suitable for non-proportional 2-D loading. McDawell, et al [13] and McNaney, et al [15] using experiments on shape memory alloys under axial torsion non-proportional loading. The obtained results proved that opposite the model based on J2 formula, in non-proportional loading, martensite strains are not in the same direction with shear stresses. This phenomena called deviate from normality (vertex effect) [11].

2.3. Constitutive Law Based on Static Constraint In this method the stress components in each micro-plane are obtained by transforming of the macro-scale stress tensor of σ_{ij} in the micro-plane. So, first the strain components of each plane are obtained using the constitutive law of the micro-plane and then the macro-scale strain tensor is obtained using the virtual work principle [11].

Stress components could be obtained as below:

$$T_i = \sigma_{ij} n_j \quad (1)$$

$$\sigma_N = \sigma_{ij} n_i n_j \quad (2)$$

$$\sigma_{si} = T_i - \sigma_N n_i \quad (3)$$

T_i is the component of stress tensor in plane and n_i is component of unit normal and σ_N is the vertical component of stress tensor and σ_{si} is the shear components of stress tensor in each micro-plane.

Based on the virtual work principle:

$$\varepsilon_{ij} = \frac{3}{2\pi}\int_{\Omega} \varepsilon_N n_i n_j d\Omega + \frac{3}{2\pi}\int_{\Omega} \frac{\varepsilon_{Sr}}{2}(n_i\delta_{rj} + n_j\delta_{ri})d\Omega \quad (4)$$

Ω is the surface of the unit hemisphere.

Equation 4 has been derived based on the fact that the virtual work inside the hemisphere and external surface is equal which has been precisely obtained by Bazant. Integral of the said equation can be derived using numerical methods of Gaussian integral with a series of points over the surface of the hemisphere. This method uses a limited series of micro-planes with different orientations for every point.

3. CONSTITUTIVE LAW ON MICRO-PLANE

The proposed constitutive law for plane has been developed upon modification of the one dimensional constitutive law presented by Sadjadpour, et al [12,19,20]. The prominent modification of this constitutive law is defining a thermo-mechanical boundary for transformation on each plane that depends on the correspond orientation of shear stress path.

3.1. Kinetic Law It is supposed that in each micro-plane, the shear strain can be divided into elastic, martensite and plastic as below:

$$\varepsilon_s(x,t) = \varepsilon_{es}(x,t) + \lambda(x,t)\varepsilon_{ms}(x,t) + \varepsilon_{ps}(x,t) \quad (5)$$

In this equation, ε_s is the total shear strain term in each micro-plane and $\lambda\varepsilon_{ms}$ is the shear strain related to the martensite phase in each micro-plane and ε_{es} is the elastic shear strain term in each micro-plane and ε_{ps} is the plastic shear strain in each micro-plane. λ represents the stress-temperature induced martensitic fraction on plane which varies between zero and one and ε_{ms} is the maximum shear strain of crystal fraction in the micro-plane that is defined as follows:

$$\varepsilon_{ms} \in \left[\varepsilon^c_{ms}, \varepsilon^t_{ms}\right] \quad \text{and} \quad \lambda \in [0,1] \quad (6)$$

Where ε^c_{ms} and ε^t_{ms} are the maximum shear strain of crystal fraction in micro-plane when the normal stress in micro-plane is of the type compression and tension, respectively. The perpendicular strain

to the micro-plane is only included in elastic transformations:

$$\varepsilon_n(x,t) = \varepsilon_{en}(x,t) \quad (7)$$

3.2. Constitutive Law The relation between shear stress and shear strain in the micro-plane is defined as follows:

$$\sigma_s = E_s(\varepsilon_s - \varepsilon_{ps} - \lambda\varepsilon_{ms}) \quad (8)$$

$$\eta = \frac{\lambda\ell}{\theta_{cr}} - C_p(1 + \mathrm{Ln}(\frac{\theta}{\theta_0})) \quad (9)$$

$$\omega(\theta) = \frac{\ell(\theta - \theta_{cr})}{\theta_{cr}} \quad (10)$$

$$d\lambda = \sigma_s\varepsilon_{ms} - \omega(\theta) \quad (11)$$

$$d\varepsilon_m = \lambda\sigma_s \quad (12)$$

$$d\varepsilon_p = \sigma_s \quad (13)$$

and the transformation in each micro-plane is defined as:

$$\dot{\lambda} = \begin{cases} \dot{\lambda}^+(1 + (d\lambda - d\lambda^+)^{-1})^{\frac{-1}{p}} & d\lambda > d\lambda^+, \lambda < 1 \\ \dot{\lambda}^-(1 + (d\lambda^- - d\lambda\lambda^{-1})^{\frac{-1}{p}} & d\lambda < d\lambda^-, \lambda > 0 \\ 0 & \text{otherwise} \end{cases} \quad (14)$$

In the above equations E_s is the shear elasticity module in micro-plane, σ_s is the shear stress component in micro-plane, η is the entropy density, ℓ is the latent heat of transformation, θ_{cr} is the thermodynamic transformation temperature, C_p is the heat capacity (assumed to be equal in both the austenite and martensite), θ_0 is the initial temperature, θ is the current temperature, $\omega(\theta)$ is the difference of chemical energy between austenite and martensite phases, $d\lambda$ is the driving force associated with the volumetric fraction in each micro-plane, $d\varepsilon_m$ is the driving force associated with the martensite strain in each micro-plane and $d\varepsilon_p$ is the driving force associated with the plastic strain in each micro-plane.

Parameters $\dot{\lambda}^+$, $\dot{\lambda}^-$, $d\lambda^+$, $d\lambda^-$ are respectively the determiner of the slope of the loop in stress-strain curve in loading path, determiner of slope of the loop in unloading path, determiner of the start point of phase transformation from austenite to martensite and determiner of the start point of phase transformation from martensite to austenite.

The term $\dot{\varepsilon}_m$ which is defined as the indicator of all the phenomena related to phase transformation such as twining, variants and detwining, the below equations are given:

$$\dot{\varepsilon}_m = K_{\varepsilon m}(d_{\varepsilon m}, \lambda, \varepsilon_m) = \frac{\alpha d_{\varepsilon m}}{\lambda} = \begin{cases} \alpha\sigma & \varepsilon_m \in \left[\varepsilon_m^c, \varepsilon_m^t\right] \\ 0 & \text{otherwise} \end{cases} \quad (15)$$

α is the parameter related to the material.

For $\dot{\varepsilon}_p$ an equation dependent to the loading rate is defined:

$$\dot{\varepsilon}_p = K_{\varepsilon p}(d_{\varepsilon p}, \sigma_y) = \frac{d_{\varepsilon p}}{H} = \begin{cases} \frac{\dot{\sigma}}{H} & \sigma \geq \sigma_{yt} \text{ or } \sigma \leq -\sigma_{yt} \\ 0 & \text{other} \end{cases} \quad (16)$$

H is the hardening parameter and σ_{yt} is the yielding shear stress. For the temperature changes the below equation is given:

$$\theta(t) = \theta_0 \exp(\frac{(\lambda(t) - \lambda_0)\ell)}{C_p\theta_{cr}}) \quad (17)$$

In each micro-plane the relations are as follows:

$$C_i = C_i^e + C_i^m + C_i^p \quad (18)$$

$$C_i^e = \begin{bmatrix} \frac{1}{E_I} & 0 \\ 0 & \frac{1}{G_I} \end{bmatrix} \quad (19)$$

$$C_i^m = \dot{\lambda} \cdot \begin{bmatrix} 0 & 0 \\ 0 & \alpha \end{bmatrix} \quad (20)$$

$$C_i^p = \begin{bmatrix} 0 & 0 \\ 0 & \frac{1}{H} \end{bmatrix} \quad (21)$$

$$\hat{C}_i = T_i \cdot C_i \cdot T_i^T \quad (22)$$

$$T_i = \left[\frac{\partial \sigma_i}{\partial \sigma} \right] \quad (23)$$

$$C = 8\pi \sum_{i=1}^{13} W_i \cdot \hat{C}_i \quad (24)$$

In the above equations, E_I and G_I are respectively the tensional and shear elasticity modules in the micro-plane and C_i is the compliance matrix in each micro-plane and C_i^e, C_i^m, C_i^p are the elasticity, phase transformation and plasticity compliance matrixes in each micro-plane respectively $\hat{C}_i$ is the transformed compliance matrix related to the i^{th} plane. T_i is the transformation matrix that transforms micro strain from micro-plane to macro-scale strain tensor. σ_i is the stress matrix in micro-plane and σ is the stress tensor in macro-scale. W_i are the weight coefficients related to the integral Equation 4 by numerical method over the surface of the hemisphere [14].

3.3. Parameters $d\lambda^+$ and $d\lambda^-$ Parameters $d\lambda^+$ and $d\lambda^-$ determine the starting point of phase transformation in a micro-plane. This has been shown in the Figure 1. In this figure, the shear path has been shown in a micro plane. Two eccentric circles with the radius $d\lambda^+$ and $d\lambda^-$ are indicators of thermo-mechanical limits of austenite and martensite phase transformations. The radiuses of these circles depend on the shear paths (22 and 23). to the extent that the thermo-mechanical path of stress does not exit the circle $d\lambda^+$, the strain is in the elastic and linear limits. As soon as the loading path passes the border of circle, martensite strains (ε_m) are started until it reaches the amount of λ to 1 in the micro-plane. In the unloading path, the strains will be linear until the reverse path of shear stress enters the circle $d\lambda^-$. In this case, the martensite strains start to return until the value of λ reaches from one to zero. In such case, all the martensite strains will return to zero. Continuing unloading the strains will return to elastic and linear case until it reaches to the initial condition i.e. zero stress and zero strain.

Values of $d\lambda^+$ and $d\lambda^-$ which indicate the starting points of phase transformation in the cases of loading and unloading respectively, are given as follows:

$$d\lambda^+ = f(a)\omega(Ms) \quad (25)$$

$$d\lambda^- = g(a)\omega(As) \quad (26)$$

in the above equations, As and Ms are the temperatures in which the transformation to austenite and martensite phase are started when the external tension is zero. f(a) and g(a) are the coefficients of micro-planes which are function of the orientation of shear stress component micro-planes (a) which has been introduced in the Section 5-2.

In the case which loading and unloading are not monotonic, i.e. the loading path change (Figure 2), at the moment of change in shear stress path in a micro-plane dependent on the angle of the direction change, another thermo-mechanical border circle to the center of the starting point of path change and the radius of the new $d\lambda^+$ can be assumed.

4. DEMONSTRATION

We now demonstrate the model by calculating the response of a material point to a given applied

stress history σ_{11} = A sin ωt and then conduct a parameter study and present capability of model.

According to the studies on a type of NiTi alloy conducted by McNaney, et al [15], parameters of material can be considered as follows:

$M_s = 51.55^{\circ}C \quad A_s = -6.36^{\circ}C$

$\ell = 12.3(J/gr) \quad C_p = 837 J/kg^{\circ}k$

$\varepsilon_c^m = -2.5\% \quad \varepsilon_t^m = 5\%$

$E = 65GPa \quad \sigma_y = 1500MPa$

Using Equations 10, 22 and 23, it leads to the following relations:

$$d\lambda^+ = f(a)\ell\left(\frac{Ms - As}{As + Ms}\right)$$

$$d\lambda^- = g(a)\ell\left(\frac{As - Ms}{As + Ms}\right) \quad (27)$$

$$\theta_{cr} = \frac{As + Ms}{2} \quad (28)$$

Now, with regard to the single axis tension as σ_{11} = A Sin ωt in which A = 1300 MPa and, ω = 2π/T and T = 5×10^{-3} s, the initial conditions are as follows:

$\varepsilon(0) = 0 \quad \varepsilon_p(0) = 0 \quad \varepsilon_m(0) = 0$

$\lambda(0) = 0 \quad \theta(0) = 0$

After comparing the results with the experiments given by McNaney [15], the parameters obtained for the material are as follows:

$a = 0 \quad \alpha = 5.65$

$f(0) = 1 \quad P = 2$

$g(0) = -0.4 \quad H = E/50$

$\dot{\lambda}^+ = -\dot{\lambda}^- = 0.1$

It should be mentioned of A < σ_y, so we will not enter the plastic strain limits. The responses resulted from micro-plane model have been shown in the Figure 3.

As loading started in an elastic state until it reaches the northwest point in the upper loop. Here, the phase transformation from austenite to martensite begins, so the slope of the curve changes. Then, it reaches the north east point in the upper loop in which the phase transformation is completed and reaches the phase of martensite completely. Again by increase of the load, it returns to the elastic state and the slope of the cure reaches the initial slope.

In the unloading path, the curve returns with this slope until it reaches to the southeast point. Here, the martensite phase begins to change to austenite phase. Continuing unloading the material is completely turned into austenite phase and it reaches to south west point in the upper loop. Then it reaches again in linear-elastic term until the tension and strain reaches zero. Similarly, for the compression loading, a loop is formed, but the tensional loop is a little different from compression loop. This phenomenon proves the asymmetry in tension and compression of alloys which can be seen in this model.

Figure 4 shows the comparison between uniaxial stress and strain which has been derived from the experimental studies conducted by Mc Naney and the curve obtained from micro-plane model.

Parameters of materials are as the same of the abovementioned ones, except for E = 40 GPa and ℓ = 8.3(J/g).

It can be clearly seen that all the curves are coincidence, only slope of curves in the reverse path is a little different in the linear-elastic term, this is due to the fact that in this model it has assumed that the elasticity module is constant in both austenite and martensite phase. It can be changed easily.

4.1. Loading Rate Figure 5 shows the uniaxial stress-strain curve with loading and unloading cycles with different rates. As it can be seen, the starting point of phase transformation does not change with stress rate increment. But because of the additional stress rate rather than martensite strain rate, hardening

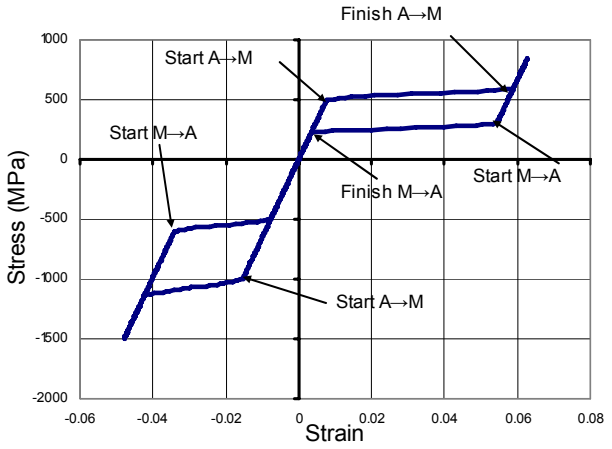

Figure 3. A typical curve of stress-strain obtained from the micro-plane model during a harmonic loading cycle.

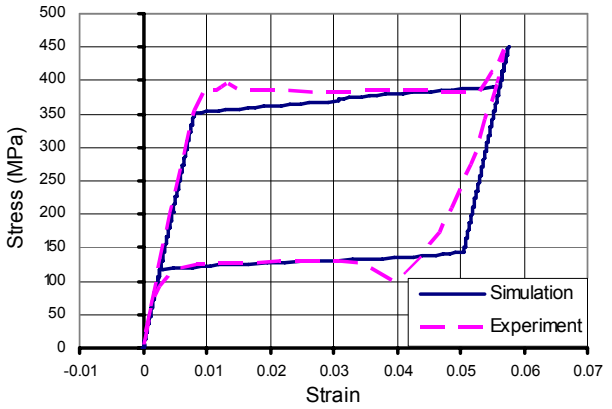

Figure 4. Comparison between micro-plane model and experimental data obtained by McNaney, et al [15] as the result of uniaxial loading and unloading.

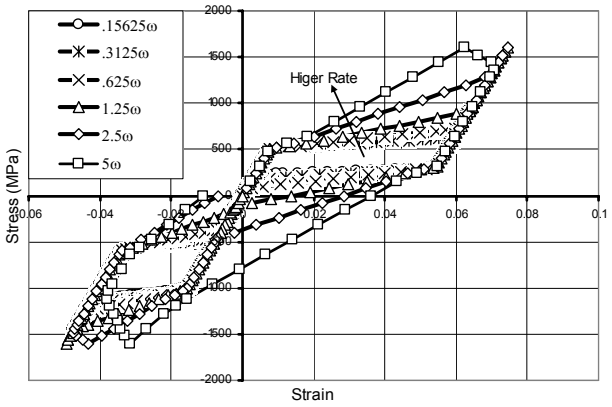

Figure 5. Numerical results related to single axis tension-strain with different rates of harmonic loading and unloading.

occurs in these curves and so an increase in the surface of loops is seen.

Also, in the higher rate of loading curve, a residual strain can be seen due to the high unloading rate. Unloading rate is so high that before the austenite phase is completed and phase transformation strains approach to zero, unloading is completed and tension reaches zero. These conditions are related to a certain stick-slip behavior that occurs due to sudden application of stresses which their corresponding strains are not fully be back after unloading. Also, in the curve related to the highest rate of loading, a softening can be seen because the loading rate is so high that before phase transformation is finished, loading reaches to pick of sinus cycle and so when unloading started, phase transformation still continues. All these results comply with experimental results [16].

4.2. Ambient Temperature and Investigating the Shape Memory Effect Figure 6 shows the temperature variations effects in stress-strain curves. In this case, different environment temperatures have been assumed as the initial temperature θ_0 and the same harmonic uniaxial loading has been applied.

As it can be seen, in the curve related to the least environment temperature i.e.-70˚C the coefficient λ increases sharply to the value of 1 in which the austenite phase has been turned into martensite phase, so it is independent to the loading And ε_m results from rotation of variant. By increase of environment temperature, for increase of the volumetric fraction coefficient λ, stress increasing is required till the environment temperature reached 170˚C and the phase transformation is not seen.

All the results of this model comply with results from observation and well known Clausius-Clapeyron relation [17].

Also, by investigation of curves the shape memory effects can be perceived. As the temperature reduced to-70˚C, the λ coefficient moves to reach 1 before loading but ε_m remains zero. In other words, temperature reduction causes phase transformation without strain. If there are a little stress increments, the strain of phase transformation increases rapidly and by unloading the residual strain remains unchanged.

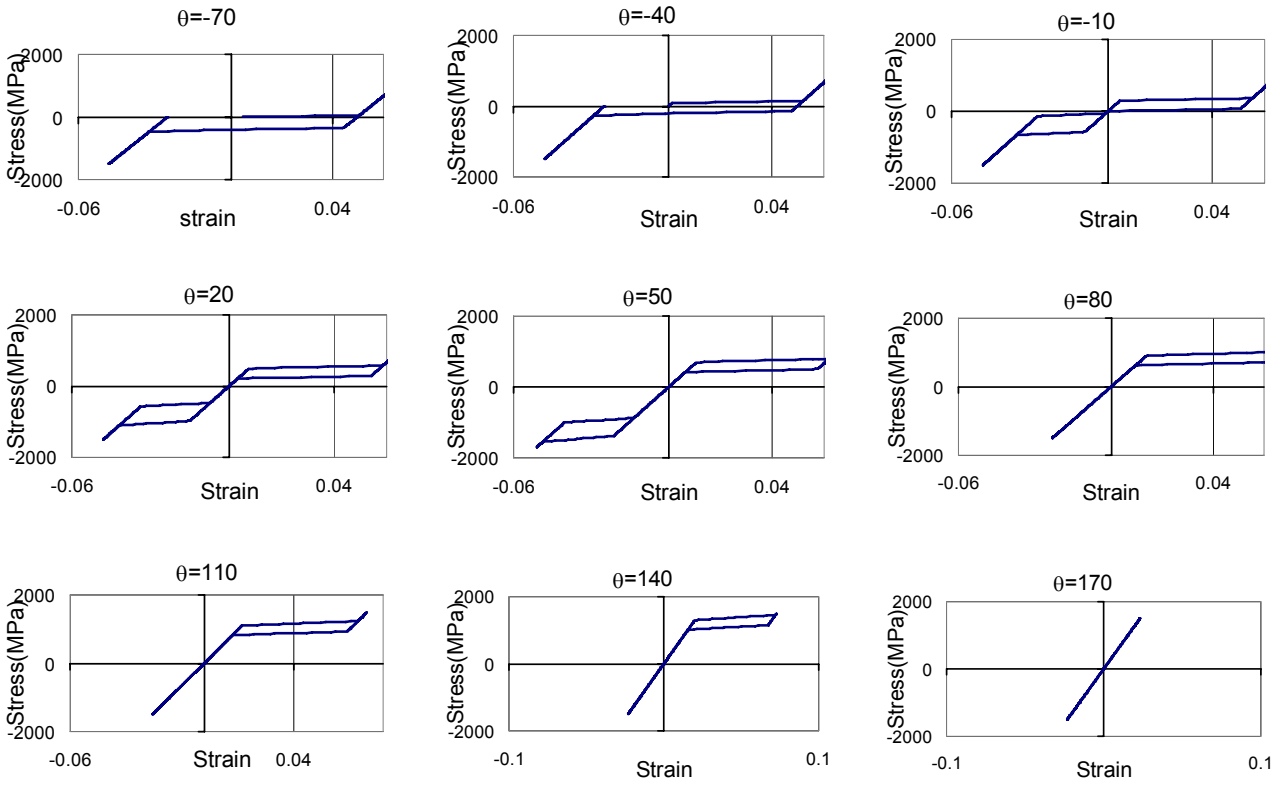

Figure 6. The numerical results of the effect of temperature changes on the single axis stress-strain curves.

But if the environment temperature increases (say 20˚C), then due to loading and unloading, no residual strain remains and as can be seen in the curve related to the temperature 20˚C, the stress related to the zero strain will be zero which actually is the shape memory effect of alloys that can be seen in this behavioral constitutive law.

4.3. Internal Loops Figure 7 shows the numerical results of the micro-plane model as the result of triangular uniaxial loading and unloading. As it can be seen, in some of these curves, before completion of the phase transformations, unloading starts, so loops become smaller and return with the same slope until the reverse phase transformation starts and the strains of the phase transformation return to their initial state and the material turns to the austenite shape. In continuation, the material returns to the same state with zero stress and strain. These curves comply with the results stated by Abeyarante, et al [18].

5. INVESTIGATION OF THE BEHAVIOR UNDER 3-D LOADING

5.1. Effects of Hydrostatic Pressure Although, the volumetric strains duo to phase transformation have been neglected in this model, but small volumetric strains have been identified in nearly all of the experimental studies [11]. These volumetric strains cause behavior of these materials to be dependent on the hydrostatic stress. This phenomenon can be seen by adding the normal

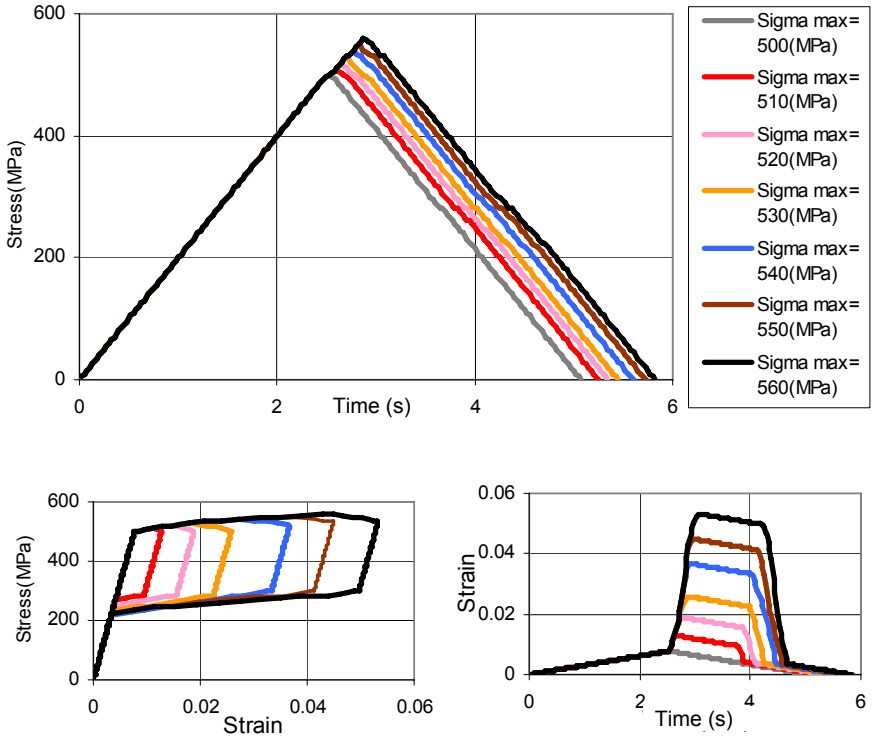

Figure 7. The numerical results of the micro-plane model as duo to triangular uniaxial loading and unloading.

effect of stress on the starting point of phase transformation in each micro-plane:

$$d\lambda^{+} = f(a)\ell\left(\frac{Ms - As}{As + Ms}\right) + f'(a)\frac{\sigma_N^2}{E_I}$$

$$d\lambda^{-} = g(a)\ell\left(\frac{As - Ms}{As + Ms}\right) - g'(a)\frac{\sigma_N^2}{E_I} \qquad (29)$$

$f'(a)$ and $g'(a)$ are the functions relating to the normal stress and a is related to the shear stress path in the micro-plane.

By comparing the curves resulted by this method in the Figure 8, the overall effect of the hydrostatic stress on the behavior of these materials can be seen. The curves are related to the effective stress $(\sigma_{11} - \sigma_{11}^{hyd})$ and effective strain $(\varepsilon_{11} - \frac{\varepsilon_v}{3})$ as the result of triangular loading and unloading of a material point in three cases. In the first case, without hydrostatic stress, loading as uniaxial tension stress and unloading to zero.

In the second case, first the point is under hydrostatic pressure of 50MPa and then the triangular uniaxial tension stress is loaded and unloaded. In the third case, the same loading is done under the hydrostatic stress of 150MPa. In all the three cases, $f'(a)$ and $g'(a)$ have been considered 0.1 but these parameters can be obtained using experimental results.

As it can be seen, by increase of the hydrostatic stress, the materials starts to phase transformation in a higher tensional stress and the loop related to the phase shift moves upward. The obtained results show qualitatively the capability of model for representing the hydrostatic pressure effects on transformation in this material.

5.2. Proportional Biaxial Loading In this section, the results obtained from the model for a single point of the material which is under simultaneous loading and unloading stress σ_{11} and shear τ_{23} has been investigated in six different cases and has been compared with experimental results obtained by McNaney, et al [15].

Six different cases of loading and unloading are as follows:

Case 1. Maximum tensional strain ε_{11} equals 6 % and maximum shear strain (torsion) ε_{23} equals 0 %

Case 2. Maximum tensional strain ε_{11} equals 6 % and maximum shear strain (torsion) ε_{23} equals 2 %

Case 3. Maximum tensional strain ε_{11} equals 3 % and maximum shear strain (torsion) ε_{23} equals 2 %

Case 4. Maximum tensional strain ε_{11} equals 1.5 % and maximum shear strain (torsion) ε_{23} equals 2 %

Case 5. Maximum tensional strain ε_{11} equals 0.7 % and maximum shear strain (torsion) ε_{23} equals 2 %

Case 6. Maximum tensional strain ε_{11} equals 0 % and maximum shear strain (torsion) ε_{23} equals 2 %

After calibration of the model with experimental results obtained by McNaney, et al [15] the values for $d\lambda^+$ and $d\lambda^-$ in each micro-plane can be introduced as a function of a based on Equations 18 and 19 in which θ is the angles between the shear stress in each micro-plane relative to the base direction. Here, the base direction is the direction of the shear stress resulting from the axis stress σ_{11} in it. These functions can be seen in the Figure 9.

In Figure 10 the obtained results have been compared with the experimental results introduced by McNaney, et al [15] in the six loading and unloading paths. As it can be seen, the results nearly coincide with each other.

5.3. Non-Proportional Biaxial Loading In this section, the results obtained from the model for a single point of the material has been presented in case the point is under single axis

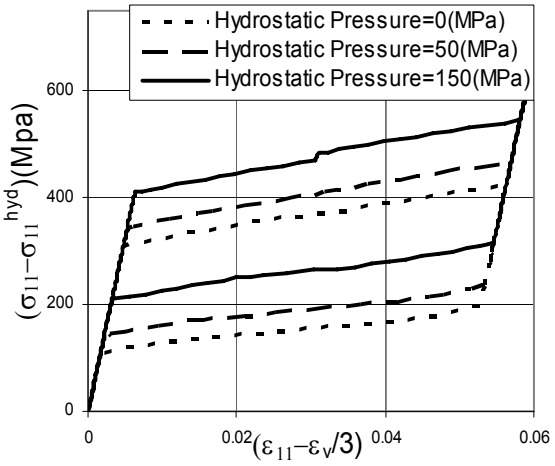

Figure 8. Effects of hydrostatic stress on the effective stress-effective strain curve obtained from micro-plane model.

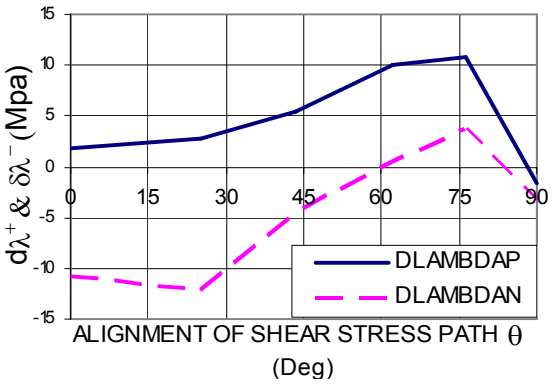

Figure 9. The changes of $d\lambda^+$ and $d\lambda^-$ relative to the angle θ.

stress in direction of σ_{11} and then shear stress is applied to it in the direction of τ_{23} as the stress σ_{11} remains constant, then shear stress unloading and tensional stress unloading is applied in three cases; The first case, the maximum tensional stress is equivalent to 0.7 % of the axial strain and the shear stress is equivalent to 2 % of the shear strain. In the second case, the figures are 1.05 % and 2 % and in the third case the figures are 6 % and 2 % respectively.

Figure 11 shows the results obtained from the micro-plane model in comparison with the experimental results obtained by McNaney, et al

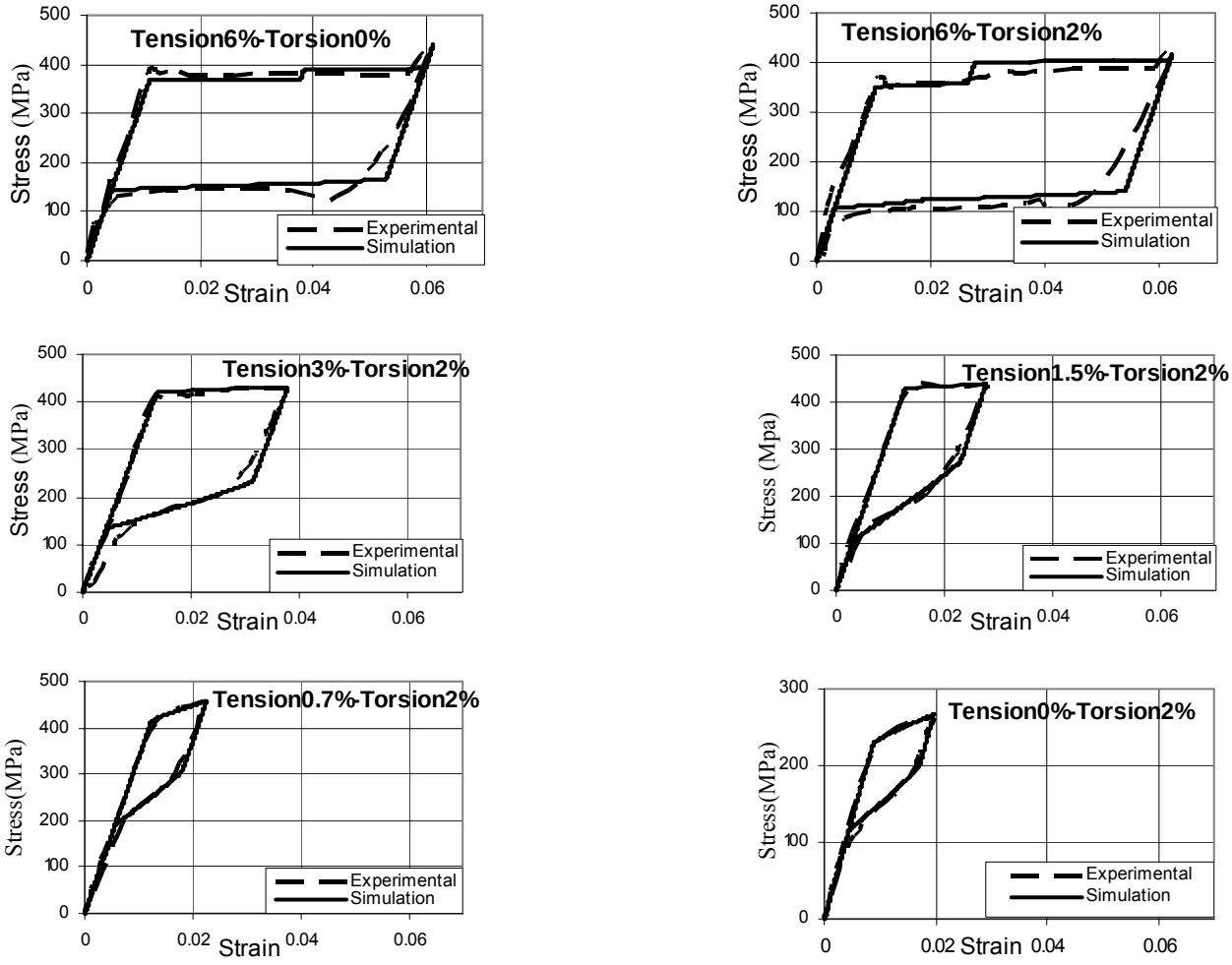

Figure 10. Comparison of the results obtained from micro-plane model with the experimental results of McNaney, et al [15] in the six paths of biaxial tensional and rotational loading and unloading.

[15], first in net rotation case and then in the three mentioned loading cases.

6. CONCLUSION

A semi-microscopic mechanical time-thermo-mechanical based model depends on loading rate, working in 3-D space developed and proposed for evaluation of shape memory alloys behavior. The micro-plane framework added this model power upon the capabilities such as applying the anisotropy effects of the non-linear behavior as well as effects resulting from the fiber-like behavior as the activity on the micro-planes. The proposed model has the ability to evaluate the asymmetry in tension and compression and hence, it presents appropriate loops in frequency of loading and unloading. The hydrostatic effect is another feature of this model. Also this model can present deviation from normality in non-proportional biaxial loading case. Results of the proposed model along with comparison with the experimental results indicate the power and capability of the proposed model. This model can be used based on the mentioned

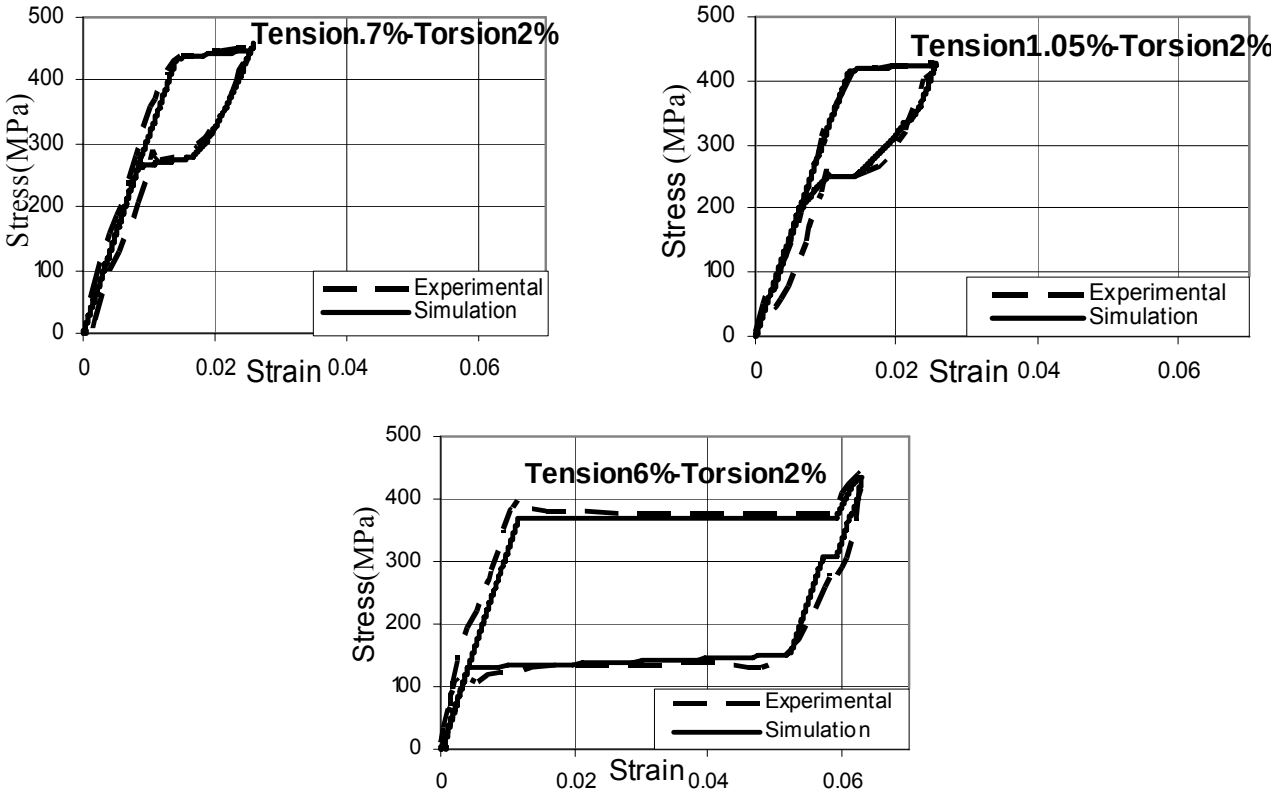

Figure 11. Comparison of the numerical results obtained from the micro-plane model and the experimental results of McNaney, et al [15] for biaxial tensional and rotational loadings.

capability in prediction of the thermo-mechanical behavior of the structures manufactured from shape memory alloys.

7. REFERENCES

1. Janke, L., Czaderski, C., Motavalli, M. and Ruth, J., "Application of Shape Memory Alloys in Civil Engineering Structures-Overview, Limits and New Ideas", ***Materials and Structures***, Vol. 38, No. 5, (June 2005), 578-592.
2. Bragg, W. L., Desch, C. H., Taylor, G. I., Mott, N. F., Orowan, E., Da, E. N., Andrade, C., Preston, G. D. and Hatfield, W. H., "A Discussion on Plastic Flow in Metals", ***Mathematical and Physical Sciences***, Vol. 168, No. 934, (7 November 1938), 302-317.
3. Batdorf, S. B. and Budiansky, B., "A Mathematical Theory of Plasticity Based on the Concept of Slip", NACA Technical Note, Vol. 1871, (April 1949).
4. Bazant, Z. P. and Prat, P. C., "Micro-Plane Model for Brittle-Plastic Material 1. Theory", ***Journal of Engineering Mechanics***, ASCE, Vol. 114, (1988), 1672-1687.
5. Bazant, Z. P., Caner, F. C., Carol, I., Adley, M. D. and Akers, S. A., "Micro-Plane Model M4 for Concrete. I: Formulation with Work-Conjugate Deviatoric Stress", ***Journal of Engineering Mechanics***, ASCE, Vol. 126, (2000), 944-953.
6. Caner, F. C. and Bazant, Z. P., "Micro-Plane Model M4 for Concrete II: Algorithm and Calibration", ***Journal of Engineering Mechanics***, ASCE, Vol. 126, (2000), 954-961.
7. Bazant, Z. P. and Prat, P. C., "Creep of Anisotropic Clay-New Micro-Plane Model", ***Journal of Engineering Mechanics***, ASCE, Vol. 113, (1987), 1050-1064.
8. Prat, P. C. and Bazant, Z. P., "Micro-Plane Model for Triaxial Deformation of Soils", ***Journal of Engineering Mechanics***, ASCE, Vol. 1989, (1989), 139-146.
9. Carol, I., Bazant, Z. P. and Prat, P. C., "Geometric

Damage Tensor Based on Micro-Plane Model", ***Journal of Engineering Mechanics***, ASCE, Vol. 117, (1991), 2429-2447.
10. Carol, I. and Bazant, Z. P., "Damage and Plasticity in Microplane Theory", ***International Journal of Solids and Structures***, Vol. 34, (1997), 3807-3835.
11. Brocca, M., Brinson, L. C. and Bazant, Z. P., "Three Dimensional Constitutive Model for Shape Memory Alloys Based on Micro-Plane", ***J. Mech. Phys. Solids***, Vol. 50, (2002), 1051-1077.
12. Sadjadpour, A. and Bhattacharya, K., "A Micromechanics Inspired Constitutive Model for Shape-Memory Alloys: The One-Dimensional Case", ***Smart Mat. Struct***., Vol. 16, (2007), 51-62.
13. Lim, T. J. and McDowell, D. L., "Mechanical Behavior of an Ni-Ti Shape Memory Alloy Under Axial-Torsional Proportional and Nonproportional Loading", ***Journal of Engineering Materials and Technology-Transaction of the ASME***, Vol. 121, No. 1, (Jan 1999), 9-18.
14. Sadrnejad, S. A., "Principles of soil plasticity", K. N. T. University, Tehran, Iran, (1999).
15. McNaney, J. M., Imbeni, V., Jung, Y., Papadopoulos, P. and Ritchie, R. O., "An Experimental Study of the Superelastic Effect in a Shape-Memory Nitinol Alloy under Biaxial Loading", ***Mechanics of Materials***, Vol. 35, (2003), 969-986.
16. Nemat-Nasser, S., Choi, J. Y., Guo, W. G. and Isaacs, J. B., "Very High Strain-Rate Response of a NiTi Shape-Memory Alloy", ***Mechanics of Materials***, Vol. 37, (2005), 287-298.
17. Otsuka, K. and Wayman, C. M., "Shape Memory Materials", Cambridge University Press, Cambridge, U.K., (1998).
18. Abeyaratne, R., Chu, C. and James, R. D., "Kinetics of Materials with Wiggly Energies: Theory and Application to the Evolution of Twinning Microstructure in a Cu-Al-Ni Alloy", ***Phil. Mag. A***, Vol. 73, (1996), 457-497.
19. Sadjadpour, A. and Bhattacharya, K., "A Micromechanics Inspired Constitutive Model for Shape Memory Alloys", ***Smart Mater***., Vol. 16, No. 5, (2007), 1751-1756.
20. Sadjadpour, A., "A Micromechanics-Inspired Three-Dimensional Constitutive Model for the Thermomechanical Response of Shape-Memory Alloys", Ph.D. Thesis, California Institute of Technology Pasadena, California, U.S.A., (2006).